Multi Modular-Rotorcraft:
An Advanced Multi-Functional and Multi-Purpose Rotorcraft

Dorsa Shirazi
Aerospace Engineer
NASA Ames Research Center
Moffett Field, CA, U.S.

Dorcas Kaweesa
Mechanical Engineer
NASA Ames Research Center
Moffett Field, CA, U.S.

ABSTRACT

The NASA Revolutionary Vertical Lift Technology project supports advanced air mobility missions through various vertical take-off and landing related projects. These efforts expand rotorcraft technology to improve the quality of life and perform "public good" missions through numerous mission concepts. The work presented herein introduces Multi Modular-Rotorcraft (MMR) technology, which explores the multifunctionality of sub-vehicles to expand the number of simultaneous missions for a rotorcraft. MMR technology can advance aeronautics through inspired transformational innovations. In this paper, the MMR concept is described, and examples of applications, 1) Disaster Relief, 2) Package Delivery, 3) Applied Science, and even 4) Planetary Exploration, are presented as potential reference missions for the MMR. With reference to an applied science mission, results from a rotor sizing demonstration and aerodynamic performance analyses of a MMR sub-vehicle, the Orb, are presented.

NOTATION

c	chord length, ft
N	number of blades
P	shaft power, hp
R	rotor radius, ft
T	thrust, lb
ρ	air density, slug/ft^3
σ	solidity
Ω	rotational speed, rad/s
C_d	drag coefficient
C_P	power coefficient
C_T	thrust coefficient
V_{tip}	tip velocity, ft/s
AAM	Advanced Air Mobility
ABL	atmospheric boundary layer
AR	aspect ratio
FM	figure of merit
GNC	Guidance, Navigation and Control
GHG	greenhouse gases
IR	Infrared radiation
LiDAR	light detection and ranging
MD	mission duration, min
MMR	Multi Modular Rotorcraft
RPM	revolutions per minute
RVLT	Revolutionary Vertical Lift Technology
TTR	twin tandem rotorcraft
UAM	Urban Air Mobility
UAV	unmanned aerial vehicles
VTOL	vertical take-off and landing

INTRODUCTION

Engineers at NASA Ames Research Center have supported projects such as the Revolutionary Vertical Lift Technology (RVLT), which aims to progress Advanced Air Mobility (AAM) goals, expand the development of vertical lift rotorcraft and Urban Air Mobility (UAM) technology [Ref. 1], and improve the quality of life through "public good" missions [Ref. 2-8]. The current state of UAM conceptual designs features a selection of rotorcraft configurations including multi-rotors, tiltrotors, quadrotors, side-by-side rotors, among others [Ref. 8], which unlock

Presented at the Vertical Flight Society's 81st Annual Forum & Technology Display, Virginia Beach, VA, USA, May 20-22, 2025.

This paper is declared a work of the U.S. Government and is not subject to copyright protection in the United States.

capabilities and opportunities for various critical service missions. The operability of such rotorcraft is contingent on factors such as structural design considerations, rotor aerodynamic performance including rotor sizing, weight requirements for payload, instrumentation, and battery pack; vehicle handling qualities, vehicle range and endurance are also important factors.

This work expands on the advancement of rotorcraft technology by introducing a Multi-Modular Rotorcraft (MMR) concept. The MMR is an advanced multi-functional and multi-purpose rotorcraft that is designed in a quadrotor configuration to disassemble into sub-vehicle and reassemble on demand into a larger comprehensive vehicle. The sub-vehicles of the MMR include the medium-sized Twin Tandem Rotorcraft (TTRs) and small-sized rotorcraft (Orbs), as shown in Figure 1. As an aggregate platform, the MMR can be designed to carry the maximum weight including all sub-vehicles, payloads, and instrumentation. With that, the MMR could collectively accomplish a wide range and diverse set of high-risk mission objectives compared to a conventional (non-modular) rotorcraft.

Each category of sub-vehicle can be tailored to operate independently or in a swarm. While on the ground, the TTRs can be reconfigured from the fully assembled quadrotor MMR by pivoting one of the TTR's rotors arms by 45° prior to flying away thus splitting into two tandem rotor vehicles. Each TTR can be designed to carry dedicated payload to support various missions. For example, TTRs can perform synchronized stereoscopic imaging of ground features by flying side-by-side. The Orbs, being the smallest sub-vehicles of the MMR, have independent navigation capabilities and can also operate in swarm-like formation to assist with mission support. The Orbs are housed in special bays within the MMR from which they are released for flight operation. The Orbs can perform aerial surveillance as well as navigate areas inaccessible by the larger MMR and TTRs.

Ultimately, mission planning for the efficient transition from MMR to TTR configuration is critical as well as the deployment and retrieval of the Orbs. Based on the desired mission, the MMR can be adapted to have optimal structural designs of the sub-vehicle components to handle the dedicated payload, efficient rotor systems which enable higher altitude and longer-range flights, and improved handling qualities for flight control. The overarching MMR concept is aspirational with regards to inspiring a whole new field of multi-rotor system design for vertical take-off and landing (VTOL) vehicles. MMR's capability to expand from a singular rotorcraft to a modular rotorcraft enables high-risk missions to be accomplished efficiently at greater success rates based on mission phase constraints.

To demonstrate the potential for developing and utilizing MMR technology, this paper presents four examples of reference missions that illustrate how MMR can be leveraged. Furthermore, the applied science application is selected for a case study in which a region of interest is identified and a mission profile for the MMR and Orbs is described. Additionally, a rotor sizing exercise is performed for a single Orb to determine the optimal rotor size and performance in terms of thrust and power required for the Orb to execute its desired mission.

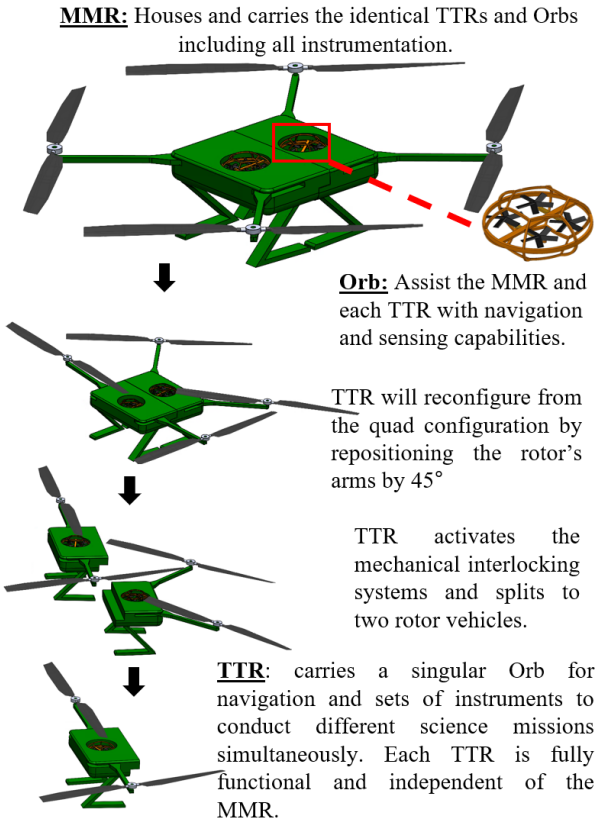

Figure 1. Preliminary MMR design and description of sub-elements.

MMR POTENTIAL APPLICATIONS

The MMR concept is neither task-specific nor invariant in size and overall configuration, making it an optimal aggregate platform for exploring different missions. While the MMR concept provides flexibility and adaptability, this section identifies four reference

missions for MMR's potential application, namely 1) Disaster Relief Efforts, 2) Package Delivery, 3) Planetary Exploration, and 4) Applied Science.

1. Disaster Relief

Disaster relief efforts refer to actions taken preemptively and in the immediate aftermath of natural disasters such as hurricanes, wildfires, earthquakes, tornadoes, and landslides. Although disaster relief actions can be implemented prior to a potential threat, it is challenging to accurately gauge the predictability and severity of natural disasters. As such, most emergency response cases focus on safe evacuations, victim recovery, and providing basic needs to affected populations during or following the catastrophe. First responders and relief workers are typically equipped with technical expertise and tools to aid in evacuations and recovery; however, in some instances, affected areas are inaccessible and restricted due to severely damaged infrastructure.

The use of unmanned aerial vehicles (UAVs) and drones has become prevalent in providing quick emergency response by delivering essential supplies in unnavigable areas, aerial surveillance for damage assessment, and scouting areas for temporary shelter for victims. While UAVs and drone technology offer various advantages in supporting disaster relief efforts, limitations such as flight endurance, limited battery life, and limited payload capacity, among others, restrict the amount of time they can spend in the air and hinder the number of supplies delivered [Ref. 8-10].

The effectiveness of the novel MMR technology is demonstrated in the ability to simultaneously deploy multiple subsystem vehicles within an affected area. The aggregate MMR platform can be launched to the site of interest and the TTRs and Orbs can be deployed hence forth within the damaged areas to survey, deliver, and collect data of the damaged areas concurrently. Both TTRs and Orbs could be equipped with Light Detection and Ranging (LiDAR), Infrared Radiation (IR) sensors, and a camera to navigate, detect, and identify victims. Compared to the larger aggregate MMR, the small-sized Orb design is advantageous because it enables flight into narrower entrances in partially collapsed buildings in the case of an earthquake, an urban fire environment, or any other natural disaster [Ref. 11, 12]. Each Orb would survey the impacted areas for stranded humans or animals and communicate with the rescue crew using the sensors onboard. MMR reduces the risk of the first responder's exposure to unsafe environments since Orbs would have surveyed the area and identified potential hazards or verified that evacuation of the people has been completed.

Some of the foreseen challenges with developing the MMR for disaster relief efforts include but aren't limited to, effective communication between the sub-vehicles, payload capacity, battery life, Guidance, Navigation and Control (GNC) subsystems, and hazard identification and assessment. However, the MMR's flexibility in sub-vehicle modification can be optimized and leveraged to effectively meet the diverse requirements of various disaster relief scenarios.

2. Package Delivery

Over the past eight years, drones have undergone significant advancements in delivering packages, including medical equipment and supplies, agricultural tools, and commercial goods, in various U.S. cities [Ref. 13]. Drone technology has advanced to ensure safe and precise delivery operations using autonomous navigation systems. Drones are equipped with sensors and cameras that make adapting to the everchanging environmental conditions easy. The sensors can assess drastic changes in weather patterns, assist with hazard avoidance, and enable visibility in low-light and foggy conditions.

With the increasing payload capacity in various industry applications, new possibilities are unlocked for MMR technology as heavy-duty drones. MMR is ideal for situations where the larger platform may replace larger delivery trucks, while the Orbs may replace hand delivery for lighter packages (less than 25 lb). In addition, the MMR can handle multiple packages whereby the TTRs and Orbs can be deployed in designated areas for different delivery tasks over varying distances.

For such implementation and the ability to handle increasing payload capacity, the aggregate MMR platform is required to maintain optimal performance for the desired duration of flight. A set of limitations with developing a MMR with sub-vehicles for package delivery include limited range, battery life that will sustain the vehicle's operation, payload capacity, and flight time, among others. As such, vehicle sizing procedures for optimal battery life and rotor performance, as well as structural design and aerodynamic analyses, should be undertaken to determine efficient performance of each vehicle.

3. Planetary Exploration

Regarding the use of rotorcraft technology for planetary exploration, Ingenuity [Ref. 14] successfully demonstrated the first powered aerodynamic flight on Mars. This capability has propelled the development of advanced rotorcraft for science investigations and mission support with dedicated payload. Whereas Ingenuity was part of an aerial and ground-based vehicle collaborative mission type with Perseverance rover, the next generation of conceptualized rotorcraft designs will be tailored to developing standalone rotorcraft such as Mars Science Helicopter [Ref. 15-19]. As such, these advanced rotorcraft's independence from a ground-based vehicle provides more opportunities for science investigations.

For planetary exploration, the MMR exemplifies an advanced standalone rotorcraft that is not only payload carrying, but also an aggregate platform that could transform into TTRs and deploy Orbs for multiple missions each carrying its own dedicated payload. Transforming into TTRs, mission profiles could be developed such that the vehicles are programmed to operate simultaneously to capture data and perform science investigations at different altitudes including scanning terrain for ice deposits, soil degradation, etc. In addition, each TTR can be designed to have additional power supply that is supplementary to the power supplied by the aggregate MMR platform. The ability to split the MMR into TTRs is advantageous because they could land in smaller landing zones, providing more accessibility. The Orbs, as the smallest sub-vehicles can be deployed to navigate narrower regions that are inaccessible to the TTRs and large MMR. Figure 2 shows the breakdown of each vehicle and the TTRs reconfiguration from MMR to a tandem configuration.

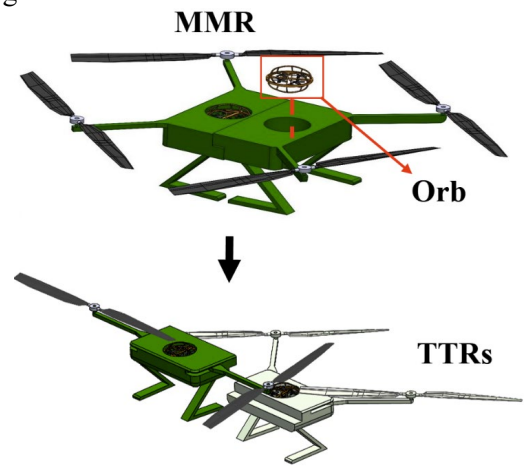

Figure 2. Schematic of MMR, the medium-size TTR, and small-size Orb vehicles.

It is important note that the schematic in Figure 2 does not reflect a final MMR design including sub-vehicle orientation. Optimal rotor structure and the appropriate number of rotor blades would have to be determined and optimized for the final MMR replica. The MMR provides numerous opportunities to aerially scan terrain and perform research and data collection for multiple science missions simultaneously over significant ranges [Ref. 14]. One major challenge with developing the MMR for extraterrestrial flight involves extensive verification and validation of each sub-vehicle and the associated subcomponents operability in the desired planetary atmosphere including determining optimal structural designs and optimized rotor aerodynamic performance.

4. Applied Science

One other area for potential application of the MMR involves applied science missions. Existing drone platforms have helped advance scientific research for instance measuring toxic plumes in air quality studies [Ref. 20], improving eruption hazard predictions in volcanic mountain studies, tracking animal populations [Ref. 21].

Depending on the science mission and associated duration, drones, whether operating individually or in a swarm, can be equipped with dedicated payload and instrumentation. Drones are also adjustable with the ability to swap payloads, if the weight limit is met, for multiple mission execution. The MMR links both capabilities, whereby it is comprehensive of a swarm and an aggregate platform.

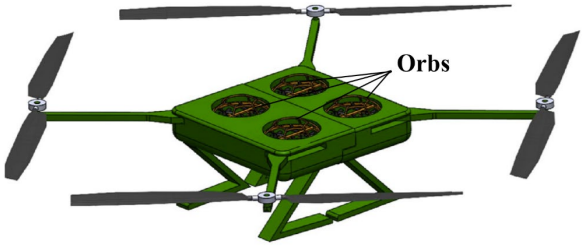

Figure 3. Design concept of MMR with multiple Orbs.

On the other hand, the Orbs' (Figure 3) ability to operate as a swarm enhances their effectiveness in comprehensively surveying the terrain. Like small drones, the small-sized Orbs have minimal impact on airflow dynamics, making them particularly advantageous for missions that necessitate reduced flow disruption. Figure 4 shows an example of Orbs performing aerial surveillance. The diagonal formation

of the Orbs' flight is essential as it limits the effect of the downwash experienced by each Orb from the other Orb's rotors. This may further impact the data collected by the sensors on board during flight operation. Additionally, the MMR platform is beneficial for conducting environmental monitoring and making localized assessments of climate change impacts.

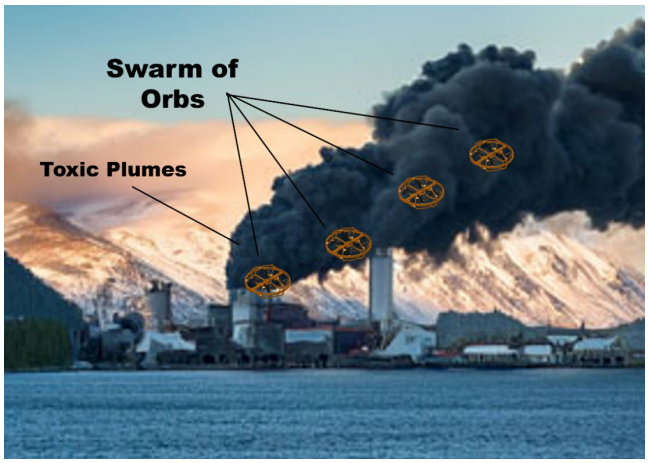

Figure 4. Swarm of Orbs performing aerial surveys to monitor air quality.

Refining the MMR for potential mission applications involves determining the payload capacity required for the desired mission, the corresponding sub-vehicles suitable for the task, the mission profile, and the anticipated duration of flight operation. Various parameters pertaining to vehicle development would then be prioritized, such as rotor sizing and aerodynamic performance, weight management of payload and instrumentation, autonomy through navigation, remote sensing capabilities, surface operations, and robotics, among others. As part of the work presented in this paper, an applied science-related mission was selected to demonstrate how the MMR, particularly the Orb sub-vehicles, can be integrated and developed for mission support.

APPLIED SCIENCE APPLICATION STUDY

In this section, the MMR concept was adapted for a notional applied science mission. Following a bottom-up approach in terms of design and analysis, the Orb was selected for further investigation since it is the smallest sub-vehicle of the MMR. The goal for this study, therefore, was to develop a vehicle concept of a single Orb for potential application in an applied science mission. The applied science mission focused on aiding in terrain surveillance and air quality measurements. In the subsequent sub-sections, a mission description for science investigation is described, and a preliminary design of the Orb is presented. Additionally, a case study for the Orb's rotor sizing and aerodynamic performance analysis is presented.

1. Mission Description for Applied Science

For the applied science application, this study focused on the region of Tanana in the western interior of Alaska and the Tanana Flats region in the Tanana River Vally lowlands of Alaska [Ref. 22]. The region of Tanana in Alaska ranges from approximately 55m to 253m in elevation and is known for its significant climatic variations, ranging from subarctic temperatures in the winter to continental temperatures in the summer, ranging from an average of -31°F to around 72 °F [Ref. 23]. The region's temperature and elevation ranges are notable because they are atmospheric conditions required for flight and operation.

Due to the extremely cold winters, large amounts of permafrost develop, which is ground surface that contains organic matter and has remained frozen for at least two consecutive years. Permafrost thaws and decomposes due to continuously rising temperatures, leading to the release of Greenhouse Gases (GHG), primarily methane and carbon dioxide, into the atmosphere. The environmental conditions in Tanana, as described by Jorgensen et al. [Ref. 24], highlight the impact of permafrost degradation and associated ecological changes. Researchers have studied the environmental conditions in Tanana, Alaska, and the impact of GHG storage on soil and vegetation in several regions in Alaska [Ref. 25-28]. In addition, researchers and scientists have conducted climatic research to monitor the changes in atmospheric conditions and GHG emissions [Ref. 29-30]. Technology initiatives using artificial intelligence have been formed to streamline the process of carbon dioxide emission measurement and analysis through language models [Ref. 31-32]. Other initiatives have involved carbon storage techniques to capture and store carbon dioxide sustainably to prevent it from being released into the atmosphere [Ref. 33-34].

Aeronautics-related innovative technologies have been implemented to complement GHG mitigation efforts by investing in sustainable aviation fuels [Ref. 35], integrating systems into aircraft or on-ground facilities [Ref. 36], and developing new propulsion systems such as hybrid-electric engines [Ref. 37]. Additionally, UAVs or drone-like rotorcraft equipped with low-cost sensors have been used to assist in surveillance and air

quality measurements at different elevations [Ref. 38-43]. For most of these applications, an advantage of utilizing UAVs and drones is based on their capability to maneuver and accurately provide real-time monitoring at various altitudes within the atmospheric boundary layer (ABL), where most ground-atmosphere interactions occur (100 m to 3 km above sea level) except in mountainous regions [Ref. 44-45]. The use of rotorcraft technology is deemed advantageous over the traditional ground-based systems because it provides enhanced air mobility, with more comprehensive coverage for precise atmospheric surveillance in remote and difficult-to-access environments.

2. Atmospheric Conditions for Flight, and Orb Design

Based on the state-of-the-art, this work specifically explored the potential use of Orb, the MMR's sub-vehicle, to assist in the monitoring of greenhouse gas emissions in the Tanana region of Alaska. The objective, therefore, was to determine the optimal rotor geometry of a single Orb with varying rotor radii to ensure that the Orb can carry up to 2 lb of science payload, including the sensors for atmospheric measurements. The region of interest for surveillance and air quality measurements lay within the troposphere, ranging in altitude between 0 and 11 km, as shown in Figure 5. This region, in which toxic plumes and greenhouse gases are most likely to be trapped, informed the flight altitude of the Orb, ranging between 394 ft – 492 ft (120 m and 150 m). The relevant atmospheric conditions conducive to flight in the Tanana region are described in Table 1. The atmospheric density was selected based on the maximum elevation of the region.

Table 1. Atmospheric conditions for flight.

Atmospheric conditions	
ρ (slug/ft^3)	0.0022
Regional elevation range (ft)	180 - 830
Temperature (F)	41
Flight altitude (ft)	394 - 492

The Orb was designed to be equipped with at least two sensors to detect the carbon dioxide and methane levels in the atmosphere within 800 ft above sea level. The sensors selected for this study as shown in Table 2, can provide high resolution surface imagery. Arbitrary weights for each sensor are included to indicate how much each instrument would contribute to the total weight of the Orb. The LiDAR sensor and camera are also included to assist with ground hazard avoidance and image capture, respectively.

Figure 5. Atmospheric ozone layers [Ref. 44].

Table 2. Sensors carried by the Orb to enable science missions.

Instruments	Weight
LiDAR	0.048 lb
CO2 sensor	0.280 lb
Methane sensor	0.039 lb
Camera	0.511 lb

SolidWorks was used to develop the Orb's baseline layout and geometry, as shown in Figure 6. The Orb was designed with a five-bladed quadrotor system. This study considered the weight of each sensor for the vehicle's total weight requirement. The flight speeds considered were 16.4 ft/s and 32.8 ft/s based on the sensors' exposure duration requirements to collect quality data [Ref. 44] within the desired region of the troposphere.

Furthermore, for aerodynamic performance evaluation of the Orb's quadrotor system, the Comprehensive Hierarchical Aeromechanics Rotorcraft Model (CHARM) was utilized as a mid-fidelity comprehensive aerodynamic analysis tool to study rotor aerodynamics for each sub-system [Ref. 46-47].

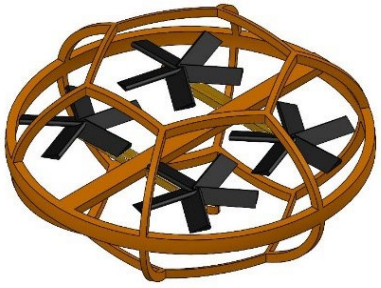

Figure 6. Preliminary Orb, small-size rotorcraft subcomponent.

3. Mission Profile for the Orb

To execute the science mission in Tanana, Alaska, a mission profile for the MMR and the Orbs combined was set up, as shown in Figure 7. The mission profile is described such that the aggregate MMR platform carrying the four Orbs, takes off and climbs to 505 ft (154 m) within the troposphere region. While the MMR is in hover at the desired elevation, the swarm of Orbs will be released to fly over the designated region for a total 15 min at a speed ranging from 16.4 ft/s – 32.8 ft/s (5 m/s - 10 m/s). The duration of flight is broken down such that the Orbs will fly and collect science data for ten minutes, and the remaining five minutes will serve as battery reserve.

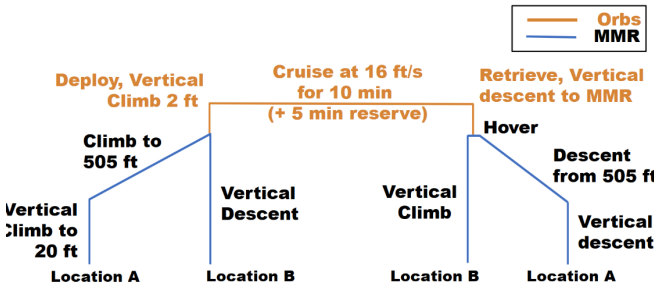

Figure 7. Mission profile.

During cruise, the Orbs perform terrain surveillance and air quality measurement in Tanana. Meanwhile, the MMR, after delivering the Orbs, will descend to ground level for about 10-15 minutes until the Orbs have completed their mission. Following the Orbs' surveillance and science measurements, the MMR will climb again and hover until the Orbs are retrieved and secured. Finally, the MMR will descend to a landing position and power off.

The purpose of the MMR in this mission profile is a means of transport for the Orbs, both to and from cruising altitude, to conserve the Orbs' battery for only flight operation during air quality measurements. It is important to note that this sample mission profile can be adapted for various science investigations within the desired region of surveillance. In addition, whereas the MMR is primarily highlighted as the Orb transporter to and from cruising altitude, the MMR's mission profile can be reconfigured for separate missions.

For this study, a single rotor of the Orb was sized to determine the optimal flight performance. Due to the small size of the Orb and the payload size constraint, the rotors are designed to be small to minimize the interruption of the toxic plumes with the motion of the rotor blades during flight. The gross weight considered for a single Orb with a quadrotor configuration was 10 lb. The mass breakdown of the subcomponents was such that the Orb carries approximately 2 lb of payload, including a total weight of 0.878 lb. (398 g) of sensors, as shown in Table 2, approximately 3 lb of battery (14.8 V), and 5 lb for the fuselage, motors, rotors, and additional instrumentation. Based on the mission profile, duration of flight, and with an assumption of downward load of 5%, a total thrust requirement of 10.5 lb was considered for the baseline rotor sizing of the Orb.

RESULTS

This section presents the results from the Orb rotor sizing and aerodynamic performance analyses. A single 4-bladed Orb rotor was modeled in CHARM with a fixed chord of 1 inch along the blade span based on the baseline size range of the Orb. Based on the atmospheric conditions presented in Table 1, additional parameters including the tip velocity and blade loading (C_T/σ) were calculated for rotors of various diameters as shown in Table 3. Since the Orb will have RPM control with fixed collective, to start the initial rotor sizing exercise, a baseline was determined by setting the rotor tip velocity to 350 ft/s. To keep the Orb size small, the rotor radius range between 2.7 inches and 3.7 inches was considered for this study. For each rotor size considered, the power requirement varied based on the motors and electronics used. This contributed to the weight of the Orb for each rotor radius. In this work, the weight of the Orb was held constant based on the payload size limitation, and the mission duration (MD) was determined for the rotor radius options.

Table 3. Sizing Parameters for the Orb blades.

Parameters	Values			
R (in)	2.7	3.0	3.5	3.7
σ	0.47	0.42	0.36	0.34
C_T	0.061	0.050	0.036	0.033
A (ft^2)	0.159	0.196	0.267	0.299
ρ (slug/ft^3)	0.0022	0.0022	0.0022	0.0022
Ω (rad/s)	1556	1400	1200	1135
V_{tip} (ft/s)	350	350	350	350
MD (min)	11	12	14	15

1. Rotor Sizing for Orb

Four cases of varying rotor radii were considered for investigation to determine the rotor(s) with the most

optimal aerodynamic performance in hover. To model the Orb's rotor blades in CHARM, the vortex lattice method was utilized along with NACA 0012 c81 table. Each data point presented in this paper is an average of over 50 revolutions of simulation results to mitigate the effect of unsteadiness in the solution. The NACA 0012 c81 Reynolds number was corrected [Ref. 48] to better match the Reynolds number experienced by the Orb's rotors for better power and performance prediction.

Figure 8-9 shows the Figure of Merit (FM) predictions based on blade loading and power versus thrust for four rotor radii, corresponding. For the rotor considered, the ideal blade loading of approximately 0.11 was used to size the Orb blade accordingly. As such, the total blade area was calculated by considering C_T/σ= 0.11, for different numbers of blades to find a reasonable chord size for each rotor radius.

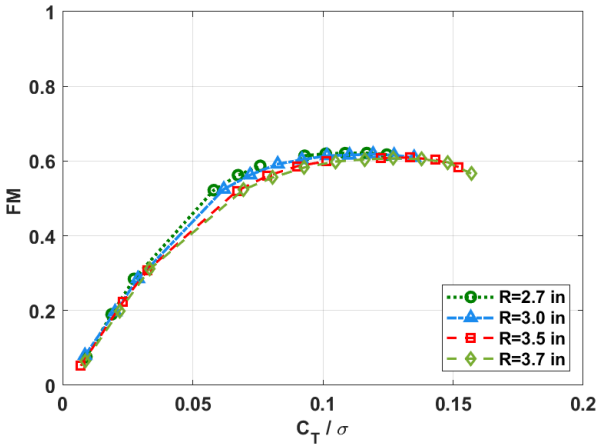

Figure 8. Single 4-bladed Orb rotor in hover – Figure of Merit vs. C_T/σ.

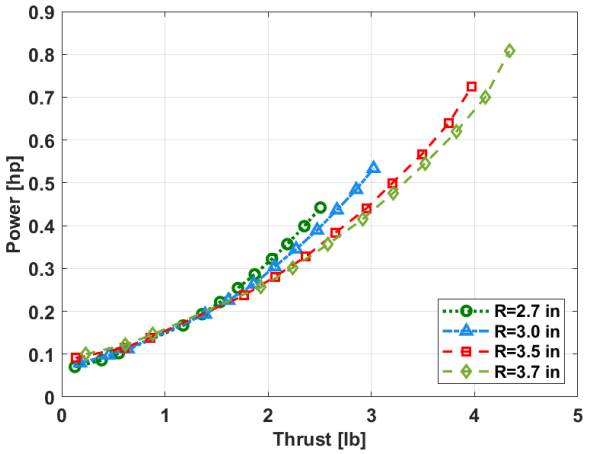

Figure 9. Single 4-bladed Orb rotor in hover– power vs. thrust.

Table 4 shows each option of rotor radius, R, blade number, N, and desired chord length, c. As observed, the largest aspect ratio (AR) can be derived for each rotor options. The 5-bladed rotor, with a radius of 3.5 inches and a chord of 0.83 inches, and the 5-bladed rotor, with a radius of 3.7 inches and a chord length of 0.80 inch, had an AR above 4, as shown in Table 5, therefore both been selected for the rotor sizing study. Additionally, the 4-bladed rotor, with a radius of 3.7 inches and a chord of 1 inch with AR=3.69 was also consider, which may be an advantage when considering the weight contribution of each blade. Table 6 shows the selected cases for the rotor sizing study.

Table 4. Rotor chord length [in] based on rotor radius and number of blades.

	R= 2.7 in	R= 3.0 in	R= 3.5 in	R= 3.7 in
N= 2	2.04	2.04	2.08	2.00
N= 3	1.36	1.36	1.39	1.33
N= 4	1.02	1.02	1.04	1.00
N= 5	0.82	0.81	0.83	0.80

Table 5. Rotor aspect ratio based on rotor radius and number of blades.

	R= 2.7 in	R= 3.0 in	R= 3.5 in	R= 3.7 in
N= 2	1.32	1.46	1.67	1.84
N= 3	1.98	2.19	2.50	2.76
N= 4	2.64	2.95	3.33	3.69
N= 5	3.30	3.64	4.17	4.61

To observe the rotor performance of the Orb's initial geometry, Table 6, each case study was modeled as an isolated rotor in free field at hover for a C_T sweep ranging from 0.002 to 0.055. Figure 10-11 shows the Figure of Merit versus bladed loading fand power versus thrust for these three selected cases.

Table 6. Rotor sizing study cases.

Parameters	**Values**		
R (inch)	3.70	3.70	3.50
c (inch)	1.00	0.80	0.83
N	4	5	5

Figures 10-11 show that the 5-bladed rotor with a radius of 3.7 inches and chord length of 0.80 inches has a high performance as the same rotor size with a chord length of 1.0 inch, while requiring a smaller power to reach the same thrust values. Therefore, the highest performing case that is, the 5-bladed rotor with a 3.7-inch radius, and a chord length of 0.80 inches was used in the initial

forward flight study cases. It is important to note that all three case studies aim to reach the C_T/σ= 0.11.

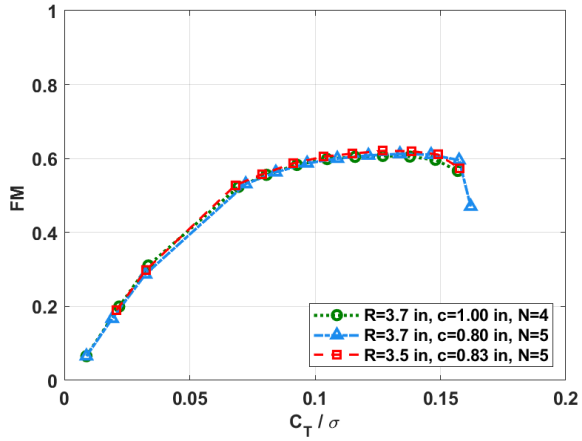

Figure 10. Orb rotor in hover trade study– Figure of Merit vs. C_T/σ.

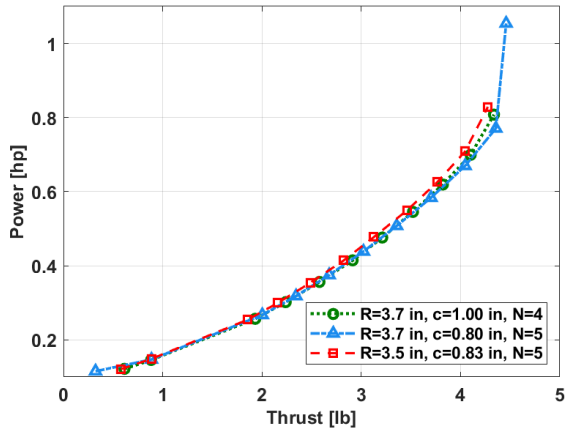

Figure 11. Orb rotor in hover – power vs. thrust.

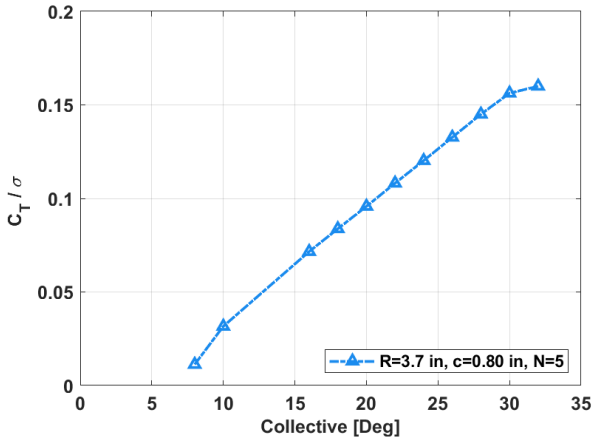

Figure 12. Orb rotor in hover – blade loading vs. collective angle.

Figure 12 shows the blade loading versus the corresponding collective angle for the 5-bladed rotor radii of 3.7 inches, and 0.8 inch chord. This result shows that the 5-bladed 3.7inch rotor reached the selected design C_T/σ= 0.11 at approximately collective 21 deg, which could be considered as a built-in collective angle at 0.75R.

a. Sweep of Linear Twist

For forward flight, rotor performance was critical to properly size the Orb's rotors, considering a cruising flight duration of 15 minutes for each mission. The forward flight speed requirement for the Orb is between 16.4-32.8 ft/s (5-10 m/s) to allow for the air quality measurements with sensors on board. Figures 13-14 show the computed total thrust and power values for front and rear rotors for the trimmed Orb vehicle. Figure 13 shows that by increasing the forward flight speed, the thrust for front rotors decreases, and for the back rotors, it increases as expected due to low Orb vehicle speed.

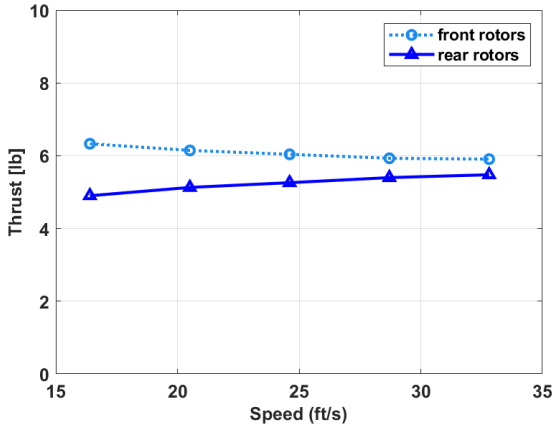

Figure 13. Orb vehicle at forward flight.

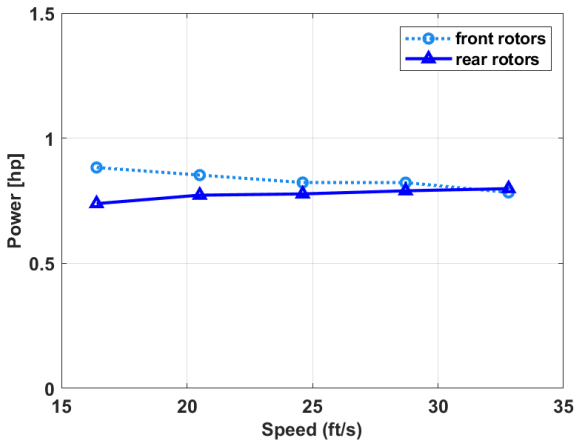

Figure 14. Orb vehicle at forward flight.

Figure 14 shows that the maximum power consumption will occur at the lowest forward flight speed of 16.4 ft/s. Additionally, trimming the Orb vehicle showed a tilt angle of -3 deg is required at 32.8 ft/s; therefore, for the

remaining forward flight cases, the forward tilt angle of 3 deg will be applied to each case study. The corresponding tip velocity of front and rear rotors from Figure 13-14 is shown on Figure 15. The minimum and maximum cruising speeds were used as an initial condition to determine the blade twist and taper for the 5-bladed 3.7-inch radius Orb rotor with a blade chord length of 0.80 inches. To better compare the power prediction between cases, each rotor was trimmed to a thrust value of 3.17 lb by adjusting the RPM. The thrust of 3.17 lb corresponds to the highest power requirements from Figure 14.

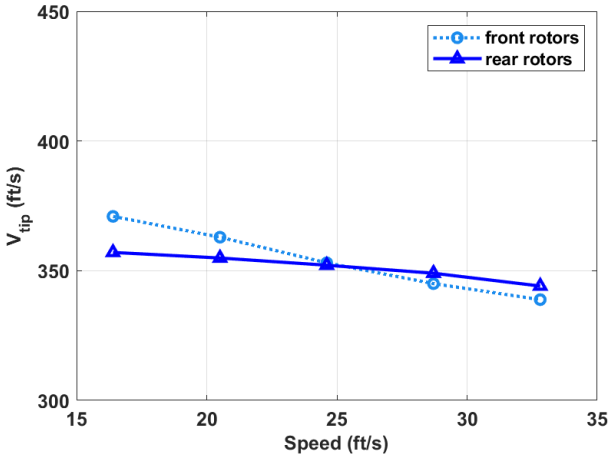

Figure 15. Orb vehicle - V_{tip} vs. forward flight speed.

Figures 16 show the rotor power predictions for the Orb at cruise speeds of 16.4 ft/s (5 m/s) and 32.8 ft/s (10 m/s) for a sweep of linear twists from -6 deg to -22 deg with increments of -2 deg.

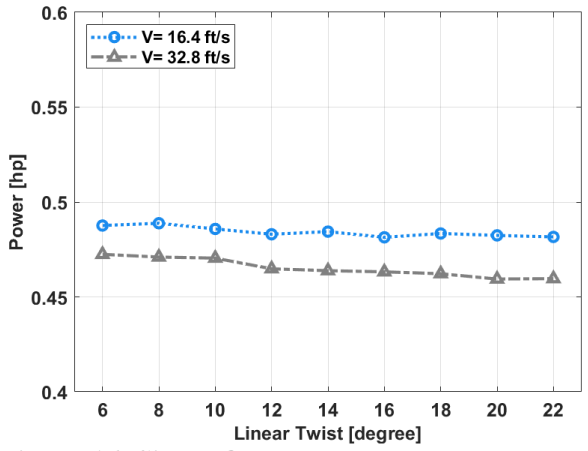

Figure 16. Single Orb rotor power versus sweep of linear twist at forward flight.

These results show that at a higher forward flight speed (32.8 ft/s), the Orb's rotor requires lower power to generate 3.17 lb of thrust, Figure17, with a minimum power value of approximately 0.459 hp, which will be associated with a linear twist of -20 deg. The RPM requirement to the corresponding power prediction from Figure 16 was shown in Figure 18 at various linear twists.

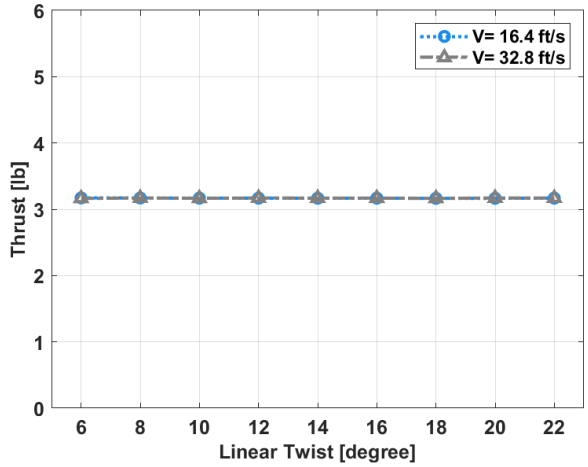

Figure 17. Single Orb rotor trimmed to thrust of 3.17 lb.

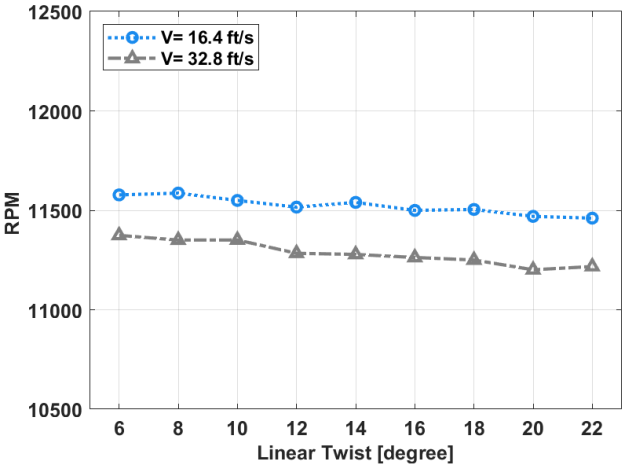

Figure 18. Single Orb rotor RPM versus sweep of linear twist at forward flight.

b. Taper and Linear Twist

To optimize the rotor geometry, linear twists and tapers were considered side by side when sizing the rotor blades. The linear twist was swept from -6 deg to -22 deg. For the taper sweep, the taper ratios of 0.6, 0.7, 0.8, 0.9, and 1.0 were applied from the rotor blade root to tip. Figures 19-20 show the variant sweep of twist and taper for the 5-bladed rotor with a 3.7-inch radius while trimming the rotor to the thrust of 3.17 lb by adjusting RPM, Figure 21. Figure 20 shows the power versus linear twist over a closer range between -16 to -22 deg

associated with the lowest power requirements, which shows that the minimum power value of approximately 0.459 hp will be associated with a linear twist range of -20 deg.

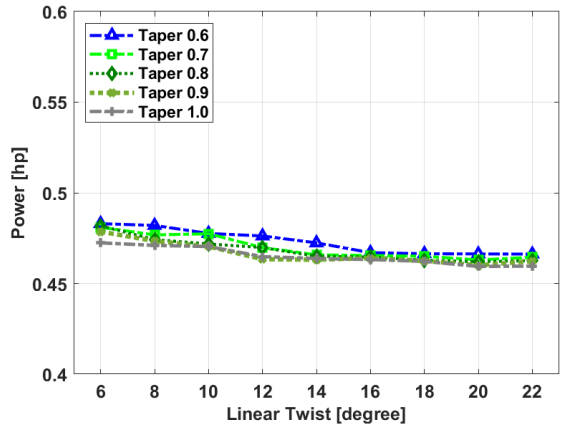

Figure 19. Orb rotor power versus twist negative deg and taper design points.

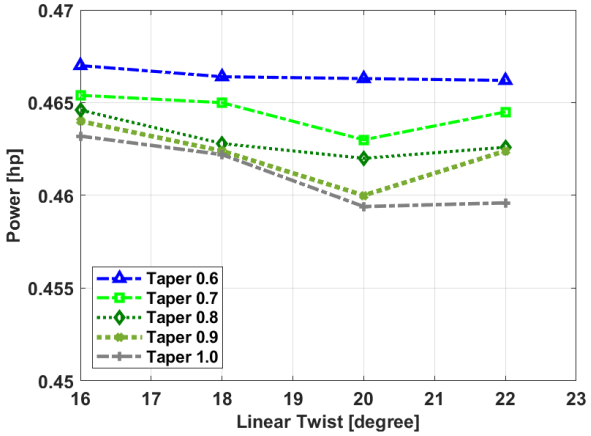

Figure 20. Orb rotor power versus twist negative deg at range of -16 to -22 deg and the taper.

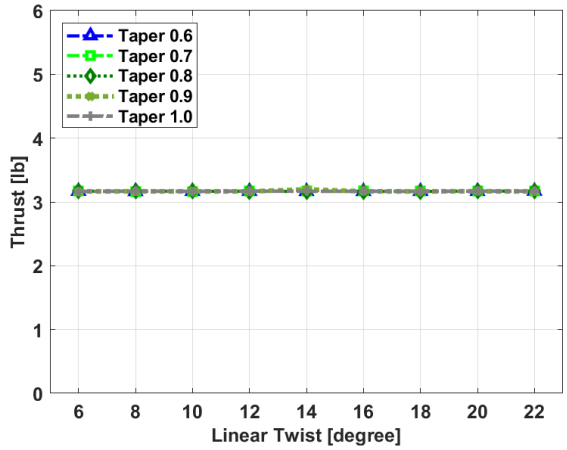

Figure 21. Orb rotor thrust versus twist and taper design points.

When comparing the power required versus the linear twist, Figure 20 shows that the rotor with a taper ratio of 1.0 (no taper, uniform chord) maintains higher rotor performance compared to the other taper ratios for each sweep of linear twist. The taper ratio of 1.0 was selected for Orb's blades, as it shows a lower power requirement of 0.459 hp for producing the same amount of thrust at a linear twist of -20 deg, Figure 20. Furthermore, the power versus required RPM was shown in Figure 22 for the 1.0 tapered case. The results show that the average lowest power requirement value for the 1.0 tapered case occurs at the RPM of 11,192.

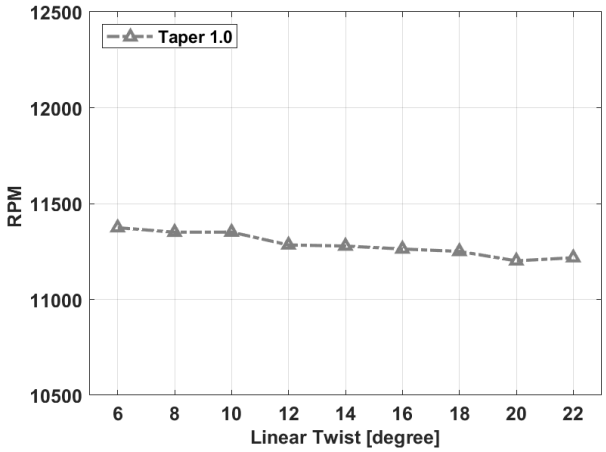

Figure 22. Orb rotor power performance at the sweep of collective angles.

2. Single Orb Rotor Performance

To further optimize the rotor geometry, the 5-bladed, 3.7-inch radius rotor was modeled with a built-in collective of 21 deg at 0.75R and a linear twist of -20 deg. Table 7 shows the power, and thrust of the Orb's rotor with a tip speed of 352 ft/s, at forward flight speeds of 16.4 ft/s and 32.8 ft/s. The results indicate that at cruise speeds of 32.8 ft/s and 16.4 ft/s, the Orb's rotor will generate 3. 17 lb and 3.01 lb of thrust, respectively.

Table 7. Rotor performance of the 5-bladed Orb rotor with a radius of 3.7 inches and linear twist of negative 20 deg and the built-in collective of 21 deg at 0.75R.

Parameters	Values	
V (ft/s)	32.8	16.4
C_T	0.037	0.035
C_P	0.0080	0.0079
T (lb)	3.17	3.01
P_{tot}(hp)	0.46	0.45

Figure 23 shows the power versus thrust generated from the single Orb rotor at a RPM sweep from 10,000 to 14,000 at forward flight speed of 32.8 ft/s.

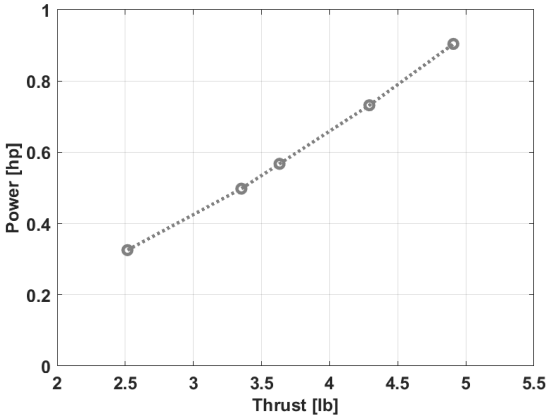

Figure 23. Orb rotor - power vs. thrust at forward speed of 32.8 ft/s.

3. Orb Rotors Performance

Following the performance analysis of the Orb's single rotor, two additional cases were analyzed with the Orb in the quadrotor configuration considering the same two forward flight speeds as before (16.4 ft/s and 32.8 ft/s). In CHARM, four 5-bladed Orb rotors with a radius of 3.7 inches and an average chord length of 0.8 inches with a taper ratio of 1.0 were modeled in an X-frame orientation. In this orientation, the tips of the rotors were 1-inch apart from one another. Also, the blades were modeled with a built-in collective angle of 21 deg at 0.75R and a linear twist of -20 deg.

Table 8 shows the total power required and thrust generated by the entire Orb quadrotor configuration at two cruise speeds of 16.4 and 32.8 ft/s. The initial gross weight for the Orb sub-vehicle was estimated to be 10 lb. The Orb in the quadrotor configuration with the current blade geometry demonstrates an average thrust of approximately 12.4 lb, at an RPM of approximately 11,100. Since the Orb vehicle has fixed collective with RPM control, further study is required to better estimate the battery, torque, and power requirements.

Table 8. Orb sub-system total power and thrust performance in forward flight.

	Thrust (lb)	Power (hp)
V=16.4 ft/s	12.04	1.62
V=32.8 ft/s	12.71	1.63

CONCLUSIONS AND FUTURE WORK

The work presented herein introduced novel multi-modular rotorcraft (MMR) technology. The MMR concept is an aggregate platform that can split into subsystems of aerial vehicles in multiple configurations. This capability unlocks various opportunities for the vehicles to be leveraged for multi-purpose missions. This paper highlights reference missions where the MMR technology can be applied and utilized, including disaster relief and emergency response efforts, package delivery services, applied science enabling missions, and missions pertaining to planetary exploration.

Considering the applied science reference mission, this work presented a concept design and trade study for the Orb, the smallest subsystem of the MMR, to determine the feasible rotor size and optimal rotor aerodynamic performance conducive for mission operation in the Tanana region in Alaska.

The mission profile for the MMR and Orbs described considered a preliminary plan of execution for the Orbs' desired science mission. As the MMR hovers at a desired elevation from where the Orbs take off, there is likely to be an effect of the MMR's rotor wake on the Orbs. As such, future work will involve additional performance analyses to ensure that the Orbs are designed with enough climb power to avoid being drafted into the downwash and outwash from the MMR. Additionally, computational fluid dynamics (CFD) analyses will be performed to investigate the rotor wake interaction between the MMR and Orbs.

Following the series of rotor sizing and performance analyses, the results indicated that the 5-bladed rotor with radius of 3.7 inches and a chord length of 0.8 inches had the best performance. Each blade has a linear twist of -20 deg with a built-in collective angle of 21 deg at 0.75R to enhance rotor performance.

Furthermore, future trade studies will optimize the Orb's blade geometry further and study the performance of rotors in different frame configurations such as X-frame, H-frame, and a hybrid frame. Additionally, generating airfoil tables for the Orb's rotor blades, considering the correct rotor size and corresponding Reynolds number, will improve the rotor performance predictions.

Author contact:

Dorsa Shirazi dorsa.shirazi@nasa.gov
Dorcas Kaweesa dorcas.kaweesa@nasa.gov

ACKNOWLEDGMENTS

The authors would like to express profound gratitude to Dr. Wayne Johnson, Michael Radotich, Dr. Nicholas Peters, Chris Silva, Dr. Sesi Kottapalli, Larry Young and Dr. Jason Cornelius for their guidance and taking the time to review and generously provide invaluable feedback. In addition, the authors would like to acknowledge Jonathan Stock, Dr. Jay Bookbinder, Laura Iraci, and Kristen Manies who inspired the applied science application study. Also, special thank you to Carl Russell, Dr. William Warmbrodt, and RVLT project for their support of this work.

REFERENCES

1. NASA Advanced Air Mobility mission; https://www.nasa.gov/mission/aam/; last accessed October 10, 2024.
2. Young, L.A., "Aerobots as a Ubiquitous Part of Society," AHS Vertical Lift Aircraft Design Conference, San Francisco, CA, January 18-20, 2006.
3. Young, L.A., "Novel Conceptual Designs for Stopped-Rotor Aerial Vehicles and Other High-Speed Rotorcraft," Sixth Decennial VFS Aeromechanics Specialists' Conference, Santa Clara, CA, Feb 6-8, 2024.
4. Young, L.A., "Urban Aerial Mobility Networks using Amphibious Vertical Takeoff and Landing Vehicles," 9th Biennial Autonomous VTOL Technical Meeting & 8th Annual Electric VTOL Symposium, Jan. 26–28, 2021
5. Young, L.A., "Future Roles for Autonomous Vertical Lift in Disaster Relief and Emergency Response," Heli-Japan 2006: AHS International Meeting on Advanced Rotorcraft Technology and Life Saving Activities, Nagoya, Japan, November 15-17, 2006.
6. Johnson, M., "Advanced Capabilities for Emergency Response Operations (ACERO)," NASA/JAXA Meeting on Disaster Response Aeronautics Research, Virtual, October 28, 2022.
7. Alonso, J.J., Arneson, H.M., Melton, J.E., Vegh, J.M., Walker, C., and Young, L.A., "System-of-Systems Considerations in the Notional Development of a Metropolitan Aerial Transportation System: Implications as to the Identification of Enabling Technologies and Reference Designs for Extreme Short Haul VTOL Vehicles with Electric Propulsion," NASA TM 2017-218356, September 2017.
8. Silva, C., Solis, E., "Aircraft Design Implications for Urban Air Mobility Vehicles Performing Public Good Missions," Vertical Flight Society's 80th Annual Forum & Technology Display, Montréal, Québec, Canada, May 7-9, 2024.
9. DeBusk, W.M., "Unmanned Aerial Vehicle Systems for Disaster Relief: Tornado Alley," Aeromechanics Branch, Flight Vehicle Research and Technology Division, 2009.
10. Conley, S., Peters, N., Aires, J., Wagner, L., Kallstrom, K., Withrow-Maser, S., Wright, S., Radotich, M., Chianello, C., Ortiz, G., Ewing, G., Anderson, A., Klokkevold, K., Kluch, E., "VTOL Analysis for Emergency Response Applications (VAERA) – Identifying Technology Gaps for Wildfire Relief Rotorcraft Missions," Vertical Flight Society Sixth Decennial Aeromechanics Specialists' Conference, Santa Clara, CA, February 2024.
11. Young, L.A., "Smart Precise Rotorcraft InTerconnected Emergency Services (SPRITES)," AIAA Science and Technology Forum and Exposition (SciTech 2018), Kissimmee, Florida, January 8-12, 2018.
12. Young, L.A., "Rotorcraft and Enabling Robotic Rescue," Heli-Japan 2010: AHS International Meeting on Advanced Rotorcraft Technology and Safety Operations, Ohmiya, Japan, Nov. 1-3, 2010.
13. Hong, F., Wu, G., Luo, Q., Liu, H., Fang, X., and Pedrycz, W., "Logistics in the Sky: A Two-Phase Optimization Approach for the Drone Package Pickup and Delivery System," IEEE Transactions on Intelligent Transportation Systems, Vol. 24, (9), 2023, pp. 9175–9190. DOI:10.1109/TITS.2023.3271430.
14. Balaram, J., Canham, T., Duncan, C., Golombek, M., Grip, H.F., Johnson, W., Maki, J., Quon, A., Stern, R., Zhu. D., "Mars helicopter technology demonstrator," AIAA Science and Technology Forum and Exposition, AIAA 2018-0023, January 2018.
15. Johnson, W., Withrow-Maser, S., Young, L., Malpica, C., Koning, W., Kuang, W., Fehler, Tuano, A., Chan, A., Datta, A., Chi, C., Lumba, R., Escobar, D., Balaram, J., Tzanetos, T., ,Grip, H., "Mars Science Helicopter Conceptual Design,"

NASA/TM—2020–220485, Moffett Field, CA, 2020
16. Kaweesa D. V., Bowman J., "Structural Analysis of Load-Bearing Components in Mars Science Helicopter," NASA/TM-2025-0000605, Moffett Field, CA, 2025.
17. Shirazi, D., Chan, A., Johnson, W., "Rotor Performance Predictions of a Next Generation Mars Science Helicopter," The Vertical Flight Society 2024 Transformative Vertical Flight, Santa Clara, CA, February 6, 2024.
18. Withrow-Maser, S., Johnson, W., Young, L., Cummings, H., Chan, A., Tzanetos, T., Balaram, J., and Bapst, J., "An Advanced Mars Helicopter Design," AIAA ASCEND Conference, Virtual, 2020.
19. Young, L.A., Aiken, E.W., Gulick, V., Mancinelli, R., and Briggs, G.A., "Rotorcraft as Mars Scouts," 2002 IEEE Aerospace Conference, Big Sky, MT, March 9-16, 2002.
20. Hayden, A. Hedworth, Tofigh Sayahi, Kerry E. Kelly, Tony Saad, "The effectiveness of drones in measuring particulate matter," *Journal of Aerosol Science*, ISSN 0021-8502, 2021.
21. Cho, R., "How Drones are Advancing Scientific Research," State of the Planet, https://news.climate.columbia.edu/2017/06/16/how-drones-are-advancing-scientific-research, June 16, 2017.
22. Nakanishi, A., and Joseph Dorava, M., "Overview of Environmental and Hydrogeologic Conditions at Tanana", Open-File Report 94-527, Anchorage, Alaska, 1994.
23. Hartman, C.W., and Johnson, "Environmental Atlas of Alaska", University of Alaska Fairbanks, Institute of Water Resources/Engineering Experiment Station, page 95, 1984.
24. Torre Jorgenson, M., Racine, C. H., Walters, J. C., Osterkamp, T. E., "Permafrost Degradation and Ecological Changes Associated with a Warming Climate in Central Alaska," *Climatic Change*. 48 (551-579), DOI:10.1023/A:1005667424292
25. O'Donnell, J. A., Harden, J. W., Manies, K. L., Torre Jorgenson, M., "Soil Data for a Collapse-Scar Bog Chronosequence in Koyukuk Flats National Wildlife Refuge, Alaska, 2008," U.S. Geological Survey Open-File Report, 2012-1230, p. 11.
26. O'Donnell, J. A., Harden, J. W., Manies, K. L., Torre Jorgenson, M., Kanevskiy, M., Xu, X., "Soil Data from Fire and Permafrost-Thaw Chronosequences in Upland Black Spruce Stands near Hess Creek and Tok, Interior Alaska," U.S. Geological Survey Open-File Report, 2013-1045, p 16.
27. Manies, K.L., Harden, J.W., and Hollingsworth, T.N., "Soils, vegetation, and woody debris data from the 2001 Survey Line fire and a comparable unburned site, Tanana Flats region, Alaska," U.S. Geological Survey Open-File Report 2014-1049, p. 36, http://dx.doi.org/10.3133/ofr20141049.
28. Manies, K.L., Harden, J.W., Fuller, C.C., Xu, X., and McGeehin, J.P., "Soil data for a vegetation gradient located at Bonanza Creek Long Term Ecological Research Site, interior Alaska," U.S. Geological Survey Open-File Report 2016–1034, p. 10, http://dx.doi.org/10.3133/ofr20161034.
29. Filonchyk, M., Peterson, M. P., Zhang, L., Hurynovich, V., He, Y., "Greenhouse Gases Emissions and Global Climate Change: Examining the Influence of CO_2, CH_4, and N_2O," *Science of The Total Environment*, 935 (173359), 2024.
30. Erland, B. M., Thorpe, A. K., Gamon, J. A., "Recent Advances Toward Transparent Methane Emissions Monitoring: A Review," *Environmental Science & Technology*. 56(23), 16567–16581, 2022.
31. Priya, A. K., Devarajan, B., Alagumalai, A., Song, H., "Artificial Intelligence Enabled Carbon Capture: A Review," *Science of The Total Environment*, 886 (163913), 2023. https://doi.org/10.1016/j.scitotenv.2023.163913.
32. Delanoe, P., Tchuente, D., Colin, G., "Method and Evaluations of the Effective Gain of Artificial Intelligence Models for Reducing CO_2 Emissions," *Journal of Environment Management*, 331(117261), 2023. https://doi.org/10.1016/j.jenvman.2023.117261
33. Bhati, A., Hamalian, M., Acharya, P., Bahadur, V., "Ultrafast Formation of Carbon Dioxide Hydrate Foam for Carbon Sequestration," *ACS Sustainable Chemistry & Engineering*, 12 (29), 2024.
34. University of Texas at Austin. "New extremely fast carbon storage technology." ScienceDaily. ScienceDaily, July 8, 2024, www.sciencedaily.com.
35. Wang, B., Ting, Z. J., Zhao, M., "Sustainable Aviation Fuels: Key Opportunities and Challenges in Lowering Carbon Emissions for Aviation Industry," *Carbon Capture Science & Technology*, 13(100263), 2024.
36. Teoh, R., Schumann, U., Voigt, C., Schripp, T., Shapiro, M., Engberg, Z., Molloy, J., Koudis, G., Stettler, M. E. J., "Targeted Use of Sustainable Aviation Fuel to Maximize Climate Benefits," *Environmental Science & Technology*, 56 (17246-17255), 2022.
37. Becattini, V., Gabrielli, P., Mazzotti, M., "Role of Carbon Capture, Storage, and Utilization to Enable

a Net-Zero CO2 Emissions Aviation Sector," *Industrial & Engineering Chemistry Research*, 60(6848-6862), 2021.
38. Johnsson, C. J. N., Drake, A., "An Assessment of Hybrid Propulsion Systems for Widebody Transport Aircraft," AIAA SciTech Forum, 2025. doi:10.2514/6.2025-1788.
39. Villa, T., Gonzalez, F., Miljievic, B., Ristovski, Z., & Morawska, L. (2016a). An overview of small unmanned aerial vehicles for air quality measurements: Present applications and future prospectives. Sensors, 16(7), 1072.
40. Villa, T. F., Salimi, F., Morton, K., Morawska, L., & Gonzalez, F. (2016b). Development and validation of a UAV based system for air pollution measurements. Sensors, 16(12), 2202.
41. Voulgarakis, A., & Field, R. D., "Fire influences on atmospheric composition, air quality and climate," *Current Pollution Reports*, 1(2), 70–81, 2015.
42. Hedworth,H.A., Sayahi, T., Kelly, E., Saad, T., "The effectiveness of drones in measuring particulate matter," *Journal of Aerosol Science*,152(1-9), 2021.
43. Rold´an, J. J., Joossen, G., Sanz, D., Del Cerro, J., Barrientos, A., "Mini-UAV based sensory system for measuring environmental variables in greenhouses. *Sensors*, 15(3334–3350), 2015.
44. Sziroczak, D., Rohacs, D., Rohacs, J., "Review of using small UAV based meteorological measurements for road weather management," *Progress in Aerospace Sciences*, 134 (100859), 2022.
45. Climate Center," Climate Change is Threatening Air Quality across the Country", Report, July 30, 2019, www.climatecentral.org.
46. Wachspress, D.A.; Quackenbush, T.R.; and Boschitsch, A.H., "Rotorcraft Interactional Aerodynamics with Fast Vortex/Fast Panel Methods," *Journal of the American Helicopter Society*, Volume 48, Number 4, 1 October 2003, pp. 223-235(13).
47. Quackenbush, T., Boschsch, A., Wachspress, D., McKillip Jr, R. and MacNichol, A., "Fast analysis methods for surface-bounded flows with applications to rotor wake modeling," American Helicopter Society 52nd Annual Forum, Washington DC, June 1996.
48. Yamauchi. G., Johnson, W., "Development and Application of an Analysis of Axisymmetric Body Effects on Helicopter Rotor Aerodynamics Using Modified Slender Body Theory", NASA Technical Memorandum 85934, July 1984.